Influence of Large Magnetic Fields on Fluorescence of Gaseous CS_2 Excited through Several V Bands

Wade N. Sisk,[†] Nilmoni Sarkar,[‡] Shigeru Ikeda,[§] and Hisaharu Hayashi*

The Institute of Physical and Chemical Research (RIKEN), Hirosawa 2-1, Wako, Saitama 351-0198, Japan

Received: April 21, 1999; In Final Form: June 21, 1999

In the present investigation, we examine fluorescence excitation spectra and fluorescence decay profiles for the 11V, 13V, 15V, and 21V bands of gaseous CS_2 under magnetic fields of up to 10 T. These experimental results indicate that the magnetic quenching (MQ) of the fluorescence from these bands can be interpreted by the hybrid of the direct and indirect mechanisms. The rotational and vibrational dependence of MQ is obtained from results of fluorescence excitation spectra. At higher fields than 1.5 T, MQ for the $K' = 1$ band (13V) exceeded that for the corresponding $K' = 0$ band (15V). From the theoretical analysis of this K' dependence, we interpret this MQ in terms of the direct mechanism. Although the vibrational dependence is not clear, this result may mean that the Zeeman interaction between V and T states is important for the direct mechanism. The dependence of MQ on J' is examined for the P(2), P(4), and P(6) lines in the 15V band. This result shows that the degree of MQ is increased with increasing J', and this trend is consistent with the previous results for other molecules.

1. Introduction

The fluorescence quenching of gaseous carbon disulfide (CS_2) by external magnetic fields (B) was discovered by Matsuzaki and Nagakura[1,2] as the first example of magnetic quenching (MQ) of the fluorescence from a nonmagnetic excited singlet state. Since this study, MQ of the fluorescence from excited singlet states in the gas phase has been widely found in many molecules at relatively small fields ($B < 2$ T) which are generated by ordinary electromagnets.[3−6] These researches have indicated that the application of a magnetic field is one of the most powerful methods to study the intramolecular radiationless transition processes of excited states. The influence of a magnetic field on the intramolecular nonradiative transition has been theoretically and systematically interpreted by two mechanisms: the indirect and direct mechanisms (IM and DM).[4−8] The MQ due to IM is caused by the field-induced acceleration of the intersystem crossing between the fluorescing singlet and isoenergetic triplet states. Such MQ has been found for many molecules: glyoxal,[9,10] acetylene,[11] formic acid,[12] pyrimidine,[13,14] and so forth.[4−6] On the other hand, MQ due to DM is caused by the field-induced acceleration of the internal conversion between the fluorescing singlet and isoenergetic other singlet states. Such MQ has been observed for a few molecules: CS_2,[1,2,15−17] sulfur dioxide,[18,19] and thiophosgene.[20]

The studies mentioned above have been performed only at $B < 2$ T with ordinary electromagnets and there has been no study on MQ under fields larger than 2 T. Even if MQ is not observable at $B < 2$ T, it is possible that MQ can be observed at $B > 2$ T. Thus, it is very interesting and important to study MQ under such large fields. Recently, Ikeda et al. have first extended external magnetic fields up to 10 T for the study of MQ and observed fluorescence excitation spectra and fluorescence decay profiles of the 6V and 10V bands of CS_2.[21] This preliminary report has given researchers new information about the intramolecular radiationless transition processes.

In the present study, we examine fluorescence excitation spectra and fluorescence decay profiles for the 11V, 13V, 15V, and 21V bands, which have one or two quanta of the bending mode (v_2') in the electronic excited state, of gaseous CS_2 under magnetic fields of up to 10 T. From these experimental results, we investigate the mechanism of MQ for these bands. Moreover, we examine the rotational (K') and vibrational (v_2') quantum number dependence of MQ, comparing fluorescence quenching ratios for various V states. From the theoretical interpretation of the rotational dependence, we discuss the mechanism of MQ in detail. Finally, we study the degree of MQ for different J' states, tuning the laser wavelength on several rotational lines of the 15V band as the magnetic field is continuously swept from 0 to 5 T.

2. Experimental Section

The experimental apparatus was identical to that utilized previously,[21] but a cell was modified for reducing scattered laser light. A superconducting magnet (SCM) system (Oxford 37057, PS120-10) was used as a magnetic field source. This magnet is capable of generating fields of up to 10 T and possesses a bore of 50 mm diameter at room temperature. The magnetic flux density (B) was measured by a gaussmeter (F. W. Bell 9200) with a hole probe (FAR92−1815). The smallest magnetic field, less than 0.2 mT, was generated by canceling the residual field with a small applied field and is designated as $B = 0$ T. A XeCl excimer laser (Lumonics EX-742) operating at 18 Hz pumped a dye laser (Lumonics HD-500) charged with DCM dye solution. This radiation was frequency doubled by an Inrad

* To whom correspondence should be addressed. Fax: 8148-462-4664. E-mail: hhayashi@postman.riken.go.jp.

[†] Present address: Chemistry Department, University of North Carolina, Charlotte, 9201 University City Blvd., Charlotte, NC 28223. Fax: 704-547-3151. E-mail: wsisk@newmail.uncc.edu.

[‡] Present address: Department of Chemistry, Indian Institute of Technology, Kharagpur, PIN: 721−302, West-Bengal, India. E-mail: nilmoni@hijli.iitkgp.ernet.in.

[§] Fax: 8148-462-4664. E-mail: ikeda@postman.riken.go.jp.

10.1021/jp991302u CCC: $18.00
Published on Web 08/20/1999

Autotracker II equipped with a KDP (KH_2PO_4) crystal and a four-prism filter that enabled separation of the second harmonic light from the fundamental. This second harmonic light had a pulse width of ca. 0.1 cm^{-1} and a pulse duration of less than 16 ns (fwhm). The direction of an electric vector of the laser light was parallel to the direction of magnetic fields. To minimize the contribution of the continuum emission,[17] the fluorescence emission was dispersed by a monochromator (Nikon P-250, reciprocal linear dispersion = 3 nm/mm) with a slit width of 100 μm. This monochromator was equipped with a photomultiplier tube (Hamamatsu R3896), which was shielded by a Permalloy and moreover held in a box made of iron plates of 10 mm thickness. Spectrograde CS_2 (Merck) was degassed by repeated freeze−pump−thaw cycles. In all spectroscopic measurements, molecules were continuously effused into a vacuum chamber placed at the cylindrical sample space of the SCM. The pressure was monitored by a capacitance manometer (Edwards Barocel Type 600AB TRANS 10 TR) and controlled by a mass flow controller with appropriate full scale (STEC SEC-400MARK3 and PAC-S5). The pressure of CS_2 was kept at 30 mTorr in all experiments. Although the fluorescence lifetime is affected by intermolecular collisions at this pressure, previous investigations showed that MQ of the CS_2 V system was independent of the pressure.[15]

Three types of experiments were performed: fluorescence excitation (FEX) spectra, fluorescence decay profiles, and sweeps of the magnetic field at fixed excitation frequency of the laser. In observations of FEX spectra, the intensity of the excitation light was simultaneously monitored in order to normalize the spectra. The emission signals were amplified by a current amplifier (SRS SR570) and then time-averaged by a boxcar integrator (SRS SR250) with gate widths of 2.0 or 6.0 μs immediately following laser excitation. The input signals to the boxcar integrator were terminated into a 1 MΩ load. The boxcar integrator was interfaced to a microcomputer for data accumulation and processing. These detection and storage systems were placed at more than 2 m from the SCM to guard against leakage of magnetic fields. The major objective of this experiment was to obtain the fluorescence quenching ratio, $S(B)/S(0\ \mathrm{T})$, where $S(B)$ is the energy integral of a FEX spectrum over a vibronic band at B. One potential problem is a drastic change of fluorescence intensities over the range, $B = 0$ to 5 T. For example, this problem was circumvented by experimentally getting $S(B_1)/S(0\ \mathrm{T})$, $S(B_2)/S(B_1)$, and $S(B_3)/S(B_2)$ for three conditions of the excitation laser and the emission detection system and the $S(B_3)/S(0\ \mathrm{T})$ value was calculated as follows:

$$S(B_3)/S(0\ \mathrm{T}) = S(B_3)/S(B_2) \times S(B_2)/S(B_1) \times S(B_1)/S(0\ \mathrm{T}) \quad (1)$$

For acquiring the fluorescence decay profiles, the emission signals were amplified by a fast voltage amplifier (SRS SR440) and then digitized by a digital storage oscilloscope (Tektronix TDS 640A) with 0.5, 5, or 10 ns per sampling point in a real time mode. The input signals into the oscilloscope were terminated in a 50 Ω load. The oscilloscope was interfaced to a microcomputer for data accumulation and processing. The jitter of a trigger signal from a photodiode was less than 3 ns. In the experiments of magnetic field sweeps, the excitation light was fixed at a particular wavelength corresponding to a particular 15V rotational line (P(2), P(4), or P(6)). The monochromator was set to the same observation wavelength utilized in the FEX spectra, the wavelength which gives maximum intensity. The magnetic field was swept at a rate of 0.17 T/min from 0 to 5 T.

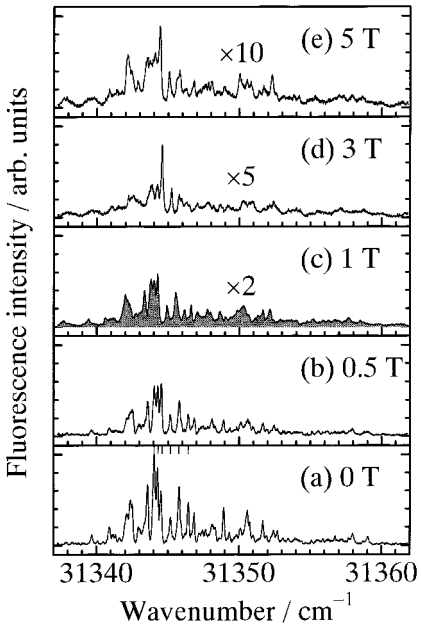

Figure 1. Fluorescence excitation spectra of the CS_2 15V band observed at room temperature for a fluorescence peak (at 24 769 cm^{-1}) under a CS_2 pressure of 30 mTorr measured at (a) $B = 0$ T, (b) $B = 0.5$ T, (c) $B = 1$ T, (d) $B = 3$ T, and (e) $B = 5$ T. In part a, the six rotationally assigned peaks designated by lines in increasing energy are P(6), P(4), P(2), R(0), R(2), and R(4).

3. Results

3.1. Fluorescence Excitation Spectra and Fluorescence Quenching Ratios. The FEX spectra of the 11V, 13V, 15V, and 21V bands of CS_2 were measured in the presence and absence of external magnetic fields. As an example, Figure 1 shows the 15V FEX spectra at different fields. As clearly shown in this figure, an extraordinary decrease in the fluorescence intensity occurs as B is increased from 0 to 5 T. There is almost no contribution of the continuum emission to the FEX spectra since we can see only discrete rotationally resolved peaks. From the jet spectroscopy of Ochi et al.,[22] the six peaks marked with lines in Figure 1a can be assigned as P(6), P(4), P(2), R(0), R(2), and R(4) in increasing energy. Inhomogeneous quenching behavior of the band is evident from the changes in relative intensities of these rotational lines in the FEX spectra from 0 to 5 T. There is no significant Zeeman broadening and shift in the resolution of the present study. In a similar way of the previous work with the 6V and 10V bands,[21] this is indicative of the acceleration of intramolecular radiationless processes by the fields. Similar magnetic field effects on the FEX spectra were also observed for the 11V, 13V, and 21V bands.

To clarify the vibronic dependence of MQ, we calculated the energy integral of an FEX spectrum, $S(B)$. Figure 1c shows how the $S(1\ \mathrm{T})$ value was obtained; the area shown by the shaded region corresponds to the $S(1\ \mathrm{T})$ value of the 15V band. The fluorescence quenching ratio, $S(B)/S(0\ \mathrm{T})$, obtained for each band with the above method is plotted against B in Figure 2. The results reported previously for the 6V and 10V bands[21] are also included for comparison in Figure 2. For each of the bands, an asymptotic decrease in $S(B)/S(0\ \mathrm{T})$ occurs as B is increased from 0 to 5 T and the fluorescence quenching ratio seems to approach zero at larger fields than 5 T. The $S(5\ \mathrm{T})/S(0\ \mathrm{T})$ values of the 11V, 13V, 15V, and 21V bands are 0.13, 0.14, 0.22, and 0.14, respectively. To examine the K' and v_2' dependence of MQ, we first show the rovibronic assignments of the excited states for all bands: 6V (0,0,0 ($K' = 1$)), 10V (0,0,0 ($K' = 0$)),

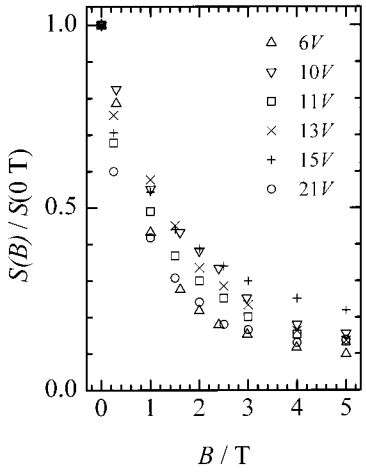

Figure 2. Magnetic field dependence of the fluorescence quenching ratios ($S(B)/S(0\ T)$) in the 6V, 10V, 11V, 13V, 15V, and 21V bands. Data for the 6V and 10V bands are taken from ref 21.

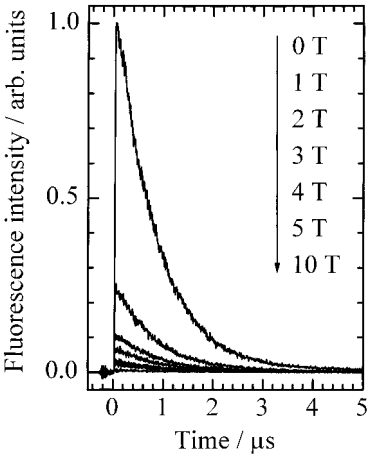

Figure 3. Fluorescence decay curves observed at room temperature with the excitation of the 13V line (at 31 199.1 cm^{-1}) and the monitor of a fluorescence peak (at 28 112 cm^{-1}) under a CS_2 pressure of 30 mTorr in the absence and presence of a magnetic field ($B = 0-10$ T). The 31 199.1 cm^{-1} line is assigned as the overlapped line of Q(1) and Q(2).

11V (unknown,1,unknown ($K' = 1$)), 13V (0,1,0 ($K' = 1$)), 15V (0,1,0 ($K' = 0$)), and 21V (0,2,0 ($K' = 0$)),[22-25] where (v_1',v_2',v_3') represents a set of the symmetric stretching, bending, and antisymmetric stretching vibration quantum numbers, respectively. The 13V and 15V bands are different from each other in only K', and we can see from Figure 2 that the fluorescence quenching ratio of the 13V($K' = 1$) band is smaller than that of the 15V($K' = 0$) one at larger fields than 1.5 T. This experimental result is consistent with that observed in the earlier work on the 6V and 10V bands; the fluorescence quenching ratio of the 6V($K' = 1$) band is smaller than that of the 10V($K' = 0$) one[21] as we can see again in Figure 2. The 10V, 15V, and 21V bands are different from one another in only v_2', but no clear v_2' dependence is found from Figure 2; the 21V($v_2' = 2$) and 10V($v_2' = 0$) bands are quenched more efficiently than the 15V($v_2' = 1$) band.

3.2. Temporal Decays. Temporal decay profiles were measured for all bands at B of up to 10 T by exciting the strongest rovibronic band in the FEX spectrum at zero field, the monochromator being fixed at each wavelength yielding a large banded-to-continuum emission ratio. The results of the 13V band are shown in Figure 3. We can see from Figure 3 that the time-integrated intensity of the decay curve is gradually decreased with increasing B from 0 to 10 T. This trend is consistent with the magnetically induced decrease in the intensity of the FEX spectrum and in the fluorescence quenching ratio, $S(B)/S(0\ T)$. Moreover, we can see that there is no fast spike, which is similar to the time profile of the excitation laser pulse, in marked contrast to time decay profiles of the 6V and 10V bands previously observed.[21] In Figure 3, the time decay profiles at $B = 0$, 1, and 2 T can be fit to single-exponential functions. Their lifetime (τ) is almost independent of B ($\tau = 0.8\ \mu s$). The time decay profiles at $B = 3$, 4, and 5 T can be fit to double-exponential functions. The lifetime of the fast decaying component is almost independent of B ($\tau = 0.8\ \mu s$). The lifetime of the slowly decaying component is also almost independent of B ($\tau = 3\ \mu s$). These double-exponential decays are dominated by the fast decaying components. Since the pre-exponent of the slowly decaying component is not almost changed by B, the slowly decaying component is attributed to the continuum emission.[17] Note that there is no magnetic field effect on the continuum emission as previously reported.[15] Consequently, we can see that the decay profile of the banded emission can be fit to a single-exponential function and that its lifetime is almost independent of B ($\tau = 0.8\ \mu s$). Similar magnetic field effects on the temporal decays were also observed for the 11V, 15V, and 21V bands.

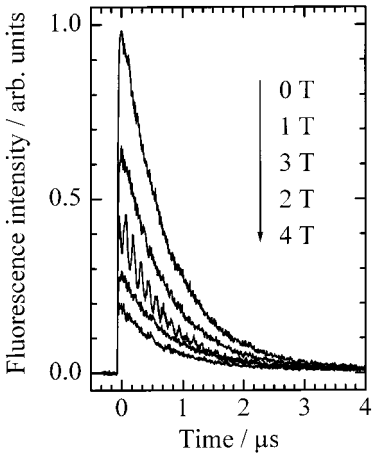

Figure 4. Fluorescence decay curves observed at room temperature with the excitation of the 15V P(2) line and the monitor of a fluorescence peak (at 24 769 cm^{-1}) under a CS_2 pressure of 30 mTorr in the absence and presence of a magnetic field ($B = 0-4$ T).

In addition, we observed the temporal decay profiles for the P(2), P(4), and P(6) rotational lines in the 15V band at various magnetic fields. As an example, the results of the P(2) excitation are shown in Figure 4. We can see from Figure 4 that the time-integrated intensity of the decay curve is not monotonically decreased with increasing B. The time-integrated intensity of the decay curve at 3 T is larger than that at 2 T. Moreover, field-induced quantum beats are observed at 3 T but not at other fields. From the Fourier transformation of quantum beat data, the beat frequency is estimated to be around 9 MHz. From the double-exponential analysis of decay profiles at fields except 3 T, it is found that every decay profile is quasi-single-exponential and that its lifetime is almost independent of B ($\tau = 0.7\ \mu s$). On the other hand, for both the P(4) and P(6) lines, it is found that the time-integrated intensity of the decay curve is monotonically decreased with increasing B and that quantum beats are not observed at any discrete values of B applied in this experiment. From the double-exponential analysis of decay profiles, it is found for both the P(4) and P(6) lines that every decay profile is quasi-single-exponential and that its lifetime is

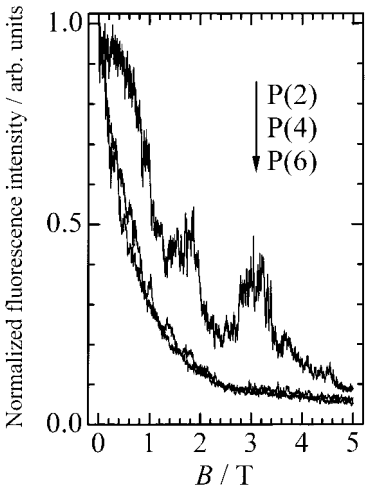

Figure 5. Normalized fluorescence intensity observed with a magnetic field sweep from 0 to 5 T for the CS_2 15V P(2), P(4), and P(6) excitation with the monitor of a fluorescence peak (at 24 769 cm^{-1}) at room temperature under a CS_2 pressure of 30 mTorr.

almost independent of B ($\tau = 0.7$ μs for the P(4) excitation and $\tau = 0.9$ μs for the P(6) excitation).

3.3. Magnetic Field Sweep. The fluorescence intensities of the P(2), P(4), and P(6) rotational lines in the 15V band were measured as B was swept from 0 to 5 T, the monochromator being fixed at 24 769 cm^{-1}. The results of all three rotational lines are shown in Figure 5, where the maximum intensity of every curve is normalized to unity. We can see from Figure 5 that the normalized fluorescence intensities (NF) are on the order of NF[P(2)] > NF[P(4)] > NF[P(6)] at every magnetic field. This means that the degree of the fluorescence quenching due to magnetic fields are on the order of P(2) < P(4) < P(6), that is, the quenching efficiencies of the fluorescence are increased with increasing J'.

Moreover, we can see from Figure 5 that each of the curves is not smooth, but that it has many peaks and valleys. However, as a whole, the fluorescence intensities of all three rotational lines seem to be decreased with increasing B and seem to be completely quenched at B larger than 5 T. Such features are consistent with the magnetically induced decrease in the time-integrated intensities of the decay profiles (vide supra). Note that the fluorescence intensity of the P(2) rotational line at 3 T is larger than that at 2 T, and this trend is consistent with the above decay result of the P(2) excitation that the time-integrated intensity of the decay curve at 3 T is larger than that at 2 T.

4. Discussion

4.1. Mechanisms of Magnetic Quenching. As mentioned above, the decay profile of the banded emission can be fit to a single-exponential function in each of the 11V, 13V, 15V, and 21V bands. This is a sharp contrast to time decay profiles of the 6V and 10V bands previously observed.[21] The decay profile of the banded emission in each of the 6V and 10V bands can be fit to a double-exponential function and, thus, the electronic relaxation processes in the 6V and 10V bands belong to the so-called "intermediate case" in the language of the radiationless transition theory.[26−28] We can safely suppose that the electronic relaxation processes in the 11V, 13V, 15V, and 21V bands also belong to the "intermediate case" as explained bellow. According to Ochi et al.,[22] the lifetime, which corresponds to the lifetime of the slowly decaying component in the banded emission, tends to become longer when CS_2 is excited to a higher vibronic level of the V state in a supersonic jet. The lifetimes of CS_2 in the nearby states, the R B_2 ($^3A_2$) and the T $^1A_2$, are on the same order of magnitude as that in the V $^1B_2$ state, although the dipole transitions from the ground state to the R and the T states are forbidden. This means that the R and the T states are strongly coupled with the V state to which the transition is dipole-allowed. Therefore, the longer lifetimes for higher vibronic levels of the V state can be attributed to higher level densities of the coupled states and/or larger interactions between the V and coupled states. From this interpretation, we can expect that the lifetime of the fast decaying component in the banded emission becomes shorter for a higher vibronic level of the V state. Since it was previously reported that the lifetime of the fast decaying component in the 6V band was 520 ps at zero fields,[17] the lifetimes in the 11V, 13V, 15V, and 21V bands at zero fields are expected to be much shorter than the duration of the excitation laser pulse, which is less than 16 ns. Consequently, we can expect that the fast decaying component does not appear in the observed decay profile so long as we use nanosecond lasers.

In a singlet state, which belongs to the "intermediate case" and the "strong coupling case",[27,28] a singlet rovibronic level ($|S\rangle$) in the zeroth-order approximation interacts with the "intermediate" dense manifold of dark triplet levels ($|T\rangle$) and approximately shows a biexponential fluorescence decay ($F(t)$):

$$F(t) = A_f \exp(-t/\tau_f) + A_S \exp(-t/\tau_S) \tag{2}$$

where τ_f and τ_S are the lifetimes of the fast and slowly decaying components, respectively, and A_f and A_S are the preexponential factors of the fast and slowly decaying components, respectively. Under a proper approximation,[28,29] τ_f and τ_S can be expressed by

$$\tau_f = \left(\frac{2\pi}{\hbar}\left|V_T\right|^2 \rho_T\right)^{-1} \tag{3}$$

$$\tau_S = \left(\frac{\gamma_S + N\bar{\gamma}_T}{\hbar(N+1)}\right)^{-1} \tag{4}$$

where ρ_T, γ_S, and $\bar{\gamma}_T$ are the state density of the triplet manifold, the line width of the $|S\rangle$, and the average line width of $|T\rangle$, respectively. Also, V_T and N are the off-diagonal matrix element coupling between $|S\rangle$ and $|T\rangle$ through the spin−orbit interaction (H_{SO}) and what is called the number of effectively coupled triplet levels, respectively, and can be expressed by

$$V_T = \langle S|H_{SO}|T\rangle \tag{5}$$

$$N = 2\pi|V_T|^2 \rho_T{}^2 \ (=\rho_T \hbar/\tau_f) \tag{6}$$

Moreover, under a proper approximation,[28,29] A_f and A_S have the following relation:

$$A_f/A_S = N \tag{7}$$

Thus, the time-integrated fluorescence intensity (I) can be given as follows:

$$I = \int_0^\infty F(t)\,dt = A_f\tau_f + A_S\tau_S = \frac{N}{N+1}\tau_f + \frac{1}{N+1}\tau_S \tag{8}$$

where we use the normalized condition, $A_f + A_S = 1$.

The MQ of gaseous fluorescence is induced by the Zeeman interaction (H_Z),

$$H_Z = -\gamma_e(\mathbf{L} + 2\mathbf{S})\cdot\mathbf{B} \tag{9}$$

in the ordinary notation. In the case of IM,[4−8] the second term of H_Z plays an important role. Since this term leads to the mixing among triplet spin sublevels, the selection rule of the spin−orbit coupling between $|S\rangle$ and $|T\rangle$ is relaxed from $\Delta J = 0$ at $B = 0$ T to $\Delta J = 0$ and ± 1 at $B \neq 0$ T, namely, the spin decoupling occurs. The spin decoupling is usually completed at a relatively small field (B_d). At $B \geq B_d$, $|V_T|^2$ and ρ_T values become as follows:

$$|V_T(B \geq B_d)|^2 = \frac{1}{3}|V_T(B = 0\ \mathrm{T})|^2 \quad (10)$$

$$\rho_T(B \geq B_d) = 3\rho_T(B = 0\ \mathrm{T}) \quad (11)$$

Thus, τ_f and N values at $B \geq B_d$ are given as follows:

$$\tau_f(B \geq B_d) = \tau_f(B = 0\ \mathrm{T}) \quad (12)$$

$$N(B \geq B_d) = 3N(B = 0\ \mathrm{T}) \quad (13)$$

From the above results and the fact that the τ_S value is almost independent of B in many molecules, in the typical case of IM, the τ_f and τ_S values are not changed by magnetic fields. Thus, the MQ due to IM is caused by the magnetically induced increase in the N value and is saturated at a relatively small field, B_d. When the second term of eq 8 is predominant and when N is much larger than 1, $I(B \geq B_d)/I(B = 0\ \mathrm{T})$ becomes $^1/_3$. This is the limiting case of IM.

In the case of DM,[4−8] the first term of H_Z plays an important role. This term leads to an additional coupling between the $|S\rangle$ level and the other singlet levels ($|S'\rangle$). To explain this case, we can rewrite the formulas of τ_f, τ_S, and N as follows:[6]

$$\tau_f = \left(\frac{2\pi}{\hbar}\left|V_T\right|^2\rho_T + \frac{2\pi}{\hbar}\left|V_S\right|^2\rho_S\right)^{-1} \quad (14)$$

$$\tau_S = \left(\frac{\gamma_S + N_T\bar{\gamma}_T + N_S\bar{\gamma}_{S'}}{\hbar(N_T + N_S + 1)}\right)^{-1} \quad (15)$$

$$N = 2\pi|V_T|^2\rho_T{}^2\,(=N_T) + 2\pi|V_S|^2\rho_S{}^2\,(=N_S) \quad (16)$$

where $\bar{\gamma}_{S'}$ and ρ_S are the average line width of the $|S'\rangle$ and the state density of $|S'\rangle$, respectively. Also, V_S is the off-diagonal matrix element directly coupling between $|S\rangle$ and $|S'\rangle$ through the Zeeman interaction and can be expressed by

$$V_S = \langle S|-\gamma_e\mathbf{L}\cdot\mathbf{B}|S'\rangle \quad (17)$$

Since B is usually directed only along one axis in the laboratory coordinates, $|V_S|^2$ is proportional to the square of B: $|V_S|^2 = \alpha B^2$. Therefore, in contrast to the case of IM, the τ_f value is changed by magnetic fields and is decreased with increasing B. Moreover, under sufficient large magnetic fields, the I value becomes almost zero because the N value becomes large enough and the τ_f value becomes nearly zero. In the case of DM, therefore, MQ can be completed at sufficiently large magnetic fields.

Previously, Imamura et al. carried out MQ studies below 1.51 T on the 6V band by using a picosecond laser.[16,17] They observed a biexponential decay in which the τ_f value was reduced upon the application of a field. This is indicative of MQ due to DM in the 6V band and, thus, the α value for the 6V band is nonzero. Note that the α value can be nonzero since the off-diagonal matrix elements of $\mathbf{L}$, $\langle V(^1B_2)|L_z(b_1)|T(^1A_2)\rangle$ and $\langle V(^1B_2)|L_x(b_2)|X(^1\Sigma_g^+)\rangle$, can be group-theoretically nonzero in the molecular coordinates where the C_2 axis is taken as y and other axis in the molecular plane is taken as z. The α value should also be nonzero for the present V bands because every V rovibronic band can be electronically coupled with the same singlet states through the Zeeman interaction. Therefore, DM is operative in MQ of the 11V, 13V, 15V, and 21V bands.

The $I(B \geq B_d)/I(B = 0\ \mathrm{T})$ ratio becomes $^1/_3$ for typical MQ due to IM as discussed above, but the ratios for several rovibronic levels of pyrazine and pyrimidine were found to be less than $^1/_3$.[14,30] The minimum value is as small as 0.15 for the P(2) line of the 12_0^2 band belonging to the $S_0 \rightarrow S_1$ transition in pyrimidine.[14] Thus, in the case of IM, the $I(B \geq B_d)$ value sometimes becomes less than $^1/_3$ of the $I(B = 0\ \mathrm{T})$ value. It is noteworthy that the $I(B \geq B_d)$ value for IM remains at a saturated value without approaching zero at large magnetic fields. In the present study, we found that the $S(5\ \mathrm{T})/S(0\ \mathrm{T})$ ratios were much less than $^1/_3$ for all bands, as seen in Figure 2, and that the $S(B)/S(0\ \mathrm{T})$ ratios seemed to approach zero with increasing B from 5 to 10 T. Moreover, the normalized fluorescence intensities of the rotational lines in the 15V band at 5 T are much less than $^1/_3$, as seen in Figure 5, and that the normalized fluorescence intensities seem to approach zero with increasing B from 5 to 10 T. Furthermore, the fluorescence of the rotational line in the 13V band is almost completely quenched at 10 T since the fluorescence decay curve at 10 T is almost completely flat, as seen in Figure 3. Such fluorescence decay results are also found for the 11V, 15V, and 21V bands. These extraordinary MQ effects observed at large magnetic fields cannot be interpreted by only IM. Consequently, our experimental results undoubtedly show that MQ in the V state has the contribution due to DM.

As we will discuss below, the evidence of the level anticrossing is included in our experimental results. This level anticrossing is caused by the spin−orbit interaction between V and $^3A_2$ states. This means that IM is operative in MQ of the V state. Thus, all the above arguments show that MQ observed in the 11V, 13V, 15V, and 21V bands is due to both DM and IM.

4.2. MQ Dependence on Nuclear Spin Statistics. As mentioned above, the fluorescence quenching ratio of the 13V($K' = 1$) band is smaller than that of the 15V($K' = 0$) one above 1.5 T. This experimental result is consistent with the previous work on the 6V and 10V bands: the fluorescence quenching ratio of the 6V($K' = 1$) band is smaller than that of the 10V($K' = 0$) one at every field.[21] Such K' dependence of MQ was previously attributed solely to selection rules for the magnetic-field-induced Zeeman coupling between the V $^1B_2$ and T $^1A_2$ levels due to DM: $\Delta J = 0, \pm 1$, $\Delta K = 0$, and $\Delta M = 0$ for $K' = 1$ and $\Delta J = \pm 1$, $\Delta K = 0$, and $\Delta M = 0$ for $K' = 0$.[21,31] Note that Fujimura et al. showed that the V−T coupling was much more important than the V−X coupling for DM.[31] A broader explanation for the preferential quenching of $K' = 1$ states can be obtained by considering nuclear spin statistics.[32] If an asymmetric-top molecule has two identical nuclei with zero spin (i.e., *boson* statistics), which is the case for $^{12}C^{32}S_2$, only those levels occur whose total wave function is symmetric with respect to an exchange of the two nuclei. Only a_1 vibrational symmetry for V states is considered because both 6V and 10V bands are vibrationless states and both 13V and 15V bands have one quantum of the totally symmetric bending vibration, υ_2'. Also, only a_1 vibrational symmetry for T states is considered because the Franck−Condon factor between V and T states should not be zero. Although the rotational eigenfunctions of an asymmetric top molecule are an appropriate linear combinations of symmetric top rotational wave functions, we use the Wang transformation[33] for convenience:

$$|J0^{+}M\rangle = |J0M\rangle \quad \text{for } K = 0 \tag{18}$$

$$|JK^{+}M\rangle = 2^{-1/2}\,(|JKM\rangle + |J{-}KM\rangle) \quad \text{for } K > 0 \tag{19}$$

$$|JK^{-}M\rangle = 2^{-1/2}\,(|JKM\rangle - |J{-}KM\rangle) \quad \text{for } K > 0 \tag{20}$$

Considering the electronic, vibrational, rotational, and nuclear symmetry, the even J levels of T states and odd J levels of V states are allowed for $K' = 0$, whereas for $K' = 1$, both even and odd J levels are allowed for both V and T states. Using the selection rules, $\Delta J = 0, \pm 1$ and $\Delta K = 0$ for $K' = 1$ and $\Delta J = \pm 1$ and $\Delta K = 0$ for $K' = 0$, matrices representing the DM-induced Zeeman coupling between V and T states can be constructed for the J values up to 7 (Tables 1 and 2). In Table 2, 1^+ and 1^- represent K^+ and K^- for $K = 1$ in the Wang transformation, respectively. We can see from these tables that the number of coupled T levels with each rovibronic level of the V($K' = 1$) state is 1.5 times larger than that of the V($K' = 0$) state. Thus, the more enhanced quenching of $K' = 1$ states than that of $K' = 0$ states is due to the greater number of the Zeeman coupled states in the $K' = 1$ state. This coupling is regulated by selection rules and nuclear spin statistics.

4.3. Level Anticrossing and Molecular Quantum Beat. The fluorescence intensities are not smoothly decreased with increasing B for the P(2), P(4), and P(6) rotational lines of the 15V band as seen in Figure 5. Previously Abe et al. also observed magnetically induced enhancement of the fluorescence from a particular rotational line of the 6V band.[17] These can be explained in terms of the level anticrossing[34] due to the spin−orbit interaction between the V and $^3A_2$ states because it was reported in previous papers that the R B_1 component of the $^3A_2$ state was strongly coupled with the V state at zero fields.[22,24] Moreover, we observe the field-induced quantum beat in the temporal decay profile for the P(2) excitation of the 15V band at 3 T as shown in Figure 4. This phenomenon is not the Zeeman quantum beat reported in previous papers[22,35] since our condition of laser excitation is the π pump, which allows the $\Delta M = 0$ transitions. Therefore, we can also interpret this phenomenon as the molecular quantum beat[34] associated with the level anticrossing due the spin−orbit interaction between the V and $^3A_2$ states.

4.4. J' and v_2' Dependence of MQ. As shown in Figure 5, the normalized fluorescence intensities (NF) of the rovibronic levels in the 15V band are on the order of NF[P(2)] > NF[P(4)] > NF[P(6)] at 0 T ≤ B ≤ 5 T. This means that the degree of MQ is increased with increasing J'. When the second term of eq 8 is predominant, N of eq 16 is much larger than 1, and τ_S is independent of B, $I(B)/I(0\ \mathrm{T})$ is given as follows:

$$\frac{I(B)}{I(0\ T)} \approx \frac{N(0\ \mathrm{T})}{N(B)} \tag{21}$$

Therefore, the J' dependence of MQ in the 15V band suggests that the ratio, $N(0\ \mathrm{T})/N(B)$ for $B > 0$ T, decreases with increasing J'. The J' dependence of MQ in the 15V band is almost consistent with that in the vibronic bands belonging to the $S_0 \rightarrow S_1$ transition in pyrazine and pyrimidine.[13,30] However, it can be seen that the states coupled with the upper level of the 15V transition are different from those of the rovibronic transitions in pyrazine and pyrimidine. While the upper levels of the rovibronic transitions in pyrazine and pyrimidine are coupled with only triplet levels through the spin−orbit interaction, those of the 15V transition are also coupled with the singlet states through the Zeeman interaction.

Previously, many researchers reported that the degree of MQ was increased as the energy of the vibronic level is increased below the predissociation threshold for the acetaldehyde S_1,[6,36] acetylene A,[11] formic acid A,[12] and sulfur dioxide C states.[18] Such vibronic energy dependence of MQ has been interpreted by the steep increase in the $N(B)$ value with the increase in the energy of the vibronic level. However, in the V state of CS_2, no clear v_2' dependence of MQ is found as shown in Figure 2. This can be caused by the irregularity in the density of states which are coupled with the V state in the presence of B. Thus, this result may support that the V−T coupling is more important than the V−X coupling for DM as mentioned above.

TABLE 1: DM-Induced Zeeman Coupling between the V $^1B_2$ and T $^1A_2$ States of CS_2 (for $K' = 0$)[a]

		V $^1B_2$ state ($K = 0$)			
	J	1	3	5	7
	0	×			
T $^1A_2$ state	2	×	×		
($K = 0$)	4		×	×	
	6			×	×

[a] The selection rule is shown as follows: $\Delta J = \pm 1$ and $\Delta K = 0$.

TABLE 2: DM-Induced Zeeman Coupling between the V $^1B_2$ and T $^1A_2$ States of CS_2 (for $K' = 1$)[a]

			V $^1B_2$ state						
	J	J $K^{\pm}$	1 1^+	2 1^-	3 1^+	4 1^-	5 1^+	6 1^-	7 1^+
	1	1^-	×	×					
	2	1^+	×	×	×				
	3	1^-		×	×	×			
T $^1A_2$ state	4	1^+			×	×	×		
	5	1^-				×	×	×	
	6	1^+					×	×	×
	7	1^-						×	×

[a] The selection rule is shown as follows: $\Delta J = 0, \pm 1$ and $\Delta K = 0$.

Acknowledgment. The authors thank Dr. Kiyoshi Nishizawa for insightful discussion about CS_2 spectroscopy. W.S. thanks the Research Development Corporation of Japan (JRDC) for the Science Technology Agency (STA) Fellowship and the National Science Foundation (NSF) for an International Travel Award. S.I. is thankful for a Grant-in-Aid (No. 09740453) for Encouragement of Young Scientists from the Ministry of Education, Science, Sports and Culture of Japan. The authors thank MR Science Project (Chemical Dynamics) of the Institute of Physical and Chemical Research (RIKEN).

References and Notes

(1) Matsuzaki, A.; Nagakura, S. *Chem. Lett.* **1974**, 675.
(2) Matsuzaki, A.; Nagakura, S. *Bull. Chem. Soc. Jpn.* **1976**, *49*, 359.
(3) Lin, S. H.; Fujimura, Y. In *Excited States*; Lim, E. C., Ed.; Academic Press: New York, 1979; Vol. 4, p 237.
(4) Steiner, U. E.; Ulrich, T. *Chem. Rev.* **1989**, *89*, 51.
(5) Hayashi, H. In *Photochemistry and Photophysics*; Rabek, J. F., Ed.; CRC Press: Boca Raton, FL, 1990; Vol. 1, p 59.
(6) Hayashi, H.; Ohta, N. In *Dynamic Spin Chemistry: Magnetic Controls and Spin Dynamics of Chemical Reactions*; Nagakura, S., Hayashi, H., Azumi, T., Ed.; Kodansha/Wiley: Tokyo/New York, 1998; p 83.
(7) Stannard, P. R. *J. Chem. Phys.* **1978**, *68*, 3932.
(8) Matsuzaki, A.; Nagakura, S. *Helv. Chim. Acta* **1978**, *61*, 675.
(9) Küttner, H. G.; Selzle, H. L.; Schlag, E. W. *Chem. Phys. Lett.* **1977**, *48*, 207.
(10) Lombardi, M.; Jost, R.; Michel, C.; Tramer, A. *Chem. Phys. Lett.* **1993**, *206*, 337.
(11) Abe, H.; Hayashi, H. *Chem. Phys.* **1992**, *162*, 225.
(12) Abe, H.; Hayashi, H. *J. Phys. Chem.* **1994**, *98*, 2797.
(13) Ohta, N.; Takemura, T.; Fujita, M.; Baba, H. *J. Chem. Phys.* **1988**, *88*, 4197.
(14) Ohta, N.; Takemura, T. *J. Chem. Phys.* **1991**, *95*, 7119.
(15) Orita, H.; Morita, H.; Nagakura, S. *Chem. Phys. Lett.* **1981**, *81*, 29.

(16) Imamura, T.; Tamai, N.; Fukuda, Y.; Yamazaki, I.; Nagakura, S.; Abe, H.; Hayashi, H. *Chem. Phys. Lett.* **1987**, *135*, 208.
(17) Abe, H.; Hayashi, H.; Imamura, T.; Nagakura, S. *Chem. Phys.* **1989**, *137*, 297.
(18) Abe, H.; Hayashi, H. *Chem. Phys. Lett.* **1991**, *187*, 227.
(19) Makarov, V. I.; Khmelinski, I. V. *J. Photochem. Photobiol. A* **1992**, *69*, 7.
(20) Lin, S. H.; Hayashi, M.; Kono, H.; Hayashi, H.; Abe, H.; Ikeda, S. *J. Chin. Chem. Soc.* **1997**, *44*, 203.
(21) Ikeda, S.; Abe, H.; Hayashi, H. *Chem. Phys. Lett.* **1996**, *257*, 507.
(22) Ochi, N.; Watanabe, H.; Tsuchiya, S.; Koda, S. *Chem. Phys.* **1987**, *113*, 271.
(23) Kleman, B. *Can. J. Phys.* **1963**, *41*, 2034.
(24) Jungen, Ch.; Malm, D. N.; Merer, A. J. *Can. J. Phys.* **1973**, *51*, 1471.
(25) Kasahara, H.; Mikami, N.; Ito, M.; Iwata, S.; Suzuki, I. *Chem. Phys.* **1984**, *86*, 173.
(26) Bixon, M.; Jortner, J. *J. Chem. Phys.* **1969**, *50*, 3284.
(27) Nitzan, A.; Jortner, J.; Rentzepis, P. M. *Proc. R. Soc. London A* **1972**, *327*, 367.
(28) Lahmani, F.; Tramer, A.; Tric, C. *J. Chem. Phys.* **1974**, *60*, 4431.
(29) Kommandeur, J.; Majewski, W. A.; Meerts, W. L.; Pratt, D. W. *Annu. Rev. Phys. Chem.* **1987**, *38*, 433.
(30) Ohta, N.; Takemura, T. *J. Chem. Phys.* **1989**, *91*, 4477.
(31) Fujimura, Y.; Hayashi, H.; Nagakura, S. *Chem. Phys.* **1992**, *162*, 205.
(32) See, for example: Herzberg, G. In *Molecular Spectra and Molecular Structure: Vol. II Infrared and Raman Spectra of Polyatomic Molecules*; Van Nostrand Reinhold: New York, 1966; Chapter IV, Section 4.
(33) Wang, S. C. *Phys. Rev.* **1929**, *34*, 243.
(34) See, for example: Dupré, P.; Jost, R.; Lombardi, M.; Green, P. G.; Abramson, E.; Field, R. W. *Chem. Phys.* **1991**, *152*, 293.
(35) Warnaar, D. L.; Silvers, S. *Chem. Phys.* **1994**, *180*, 89.
(36) Ohta, N.; Koguchi, T.; Takemura, T.; Suzuka, I. *Chem. Phys. Lett.* **1992**, *191*, 232.